Journal of Materials Chemistry A

Accepted Manuscript

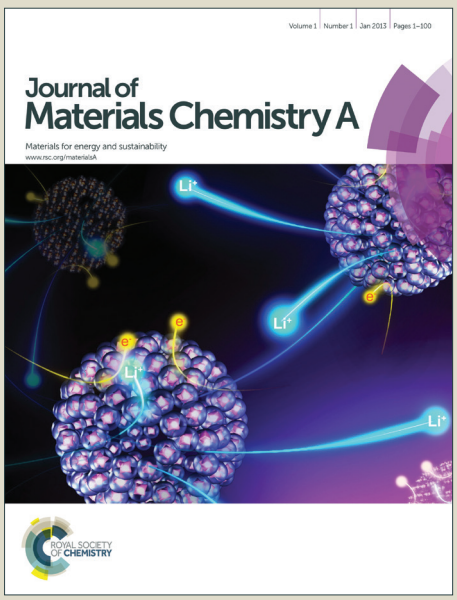

ROYAL SOCIETY OF CHEMISTRY

www.rsc.org/materialsA

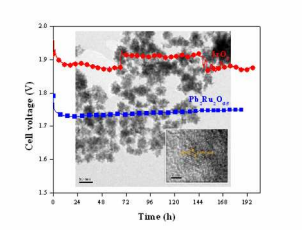

Lead ruthenate pyrochlore showed exceptional OER activity and stability when tested in a solid-state alkaline water electrolyzer.

Journal of
Materials Chemistry A

RSCPublishing

ARTICLE

Pyrochlore electrocatalysts for efficient alkaline water electrolysis

Cite this: DOI: 10.1039/x0xx00000x

Javier Parrondo[a], Morgan George[b], Christopher Capuano[b], Katherine E. Ayers[b] and Vijay Ramani[a,*]

Received 00th January 2015,
Accepted 00th January 2015

DOI: 10.1039/x0xx00000x

www.rsc.org/

A series of electrically conducting metal oxides with the pyrochlore structure ($A_2B_2O_{7-y}$, with A=Pb or Bi and B= Ru, Ir or Os) were synthesized via precipitation/crystallization in alkaline medium and/or via solid-state reaction. The electrocatalytic activity for the oxygen evolution reaction (OER) in 0.1M KOH was studied using a rotating disk electrode. Lead and bismuth ruthenate pyrochlores showed significantly lower overpotentials for the OER than the state-of-the-art IrO_2 catalyst. Specific activities (at 1.5 V vs. RHE) of 3.0±0.2 Am^{-2}, 1.3±0.2 Am^{-2} and 0.06±0.01 Am^{-2} were obtained for $Pb_2Ru_2O_{6.5}$, $Bi_{2.4}Ru_{1.6}O_7$, and IrO_2 respectively. Specific activities for iridate-based pyrochlores (0.3-0.5 Am^{-2}) were 5-10 times lower than those for ruthenate-based pyrochlores. Lead osmate pyrochlore showed the lowest OER activity among all the pyrochlores evaluated, with a specific activity of 0.10±0.07 Am^{-2}. It is proposed that the reaction path for the OER involves several oxygen intermediate species (-O^{2-}, -OOH, -OO^{2-}, -OH) bonded to the B-site (Ru, Ir or Os) in the pyrochlore, and that the catalytic activity depends on the bonding strength between the B-cation site and the oxygen species. This hypothesis was supported by the fact that OER activity correlated with Ru concentration in lead-rich lead ruthenate pyrochlores. The decrease of the specific OER activity depended on the occupancy of the 3d orbitals and on the period in the periodic table occupied by the B-cation. The OER activity decreased for pyrochlores with B cations having more d electrons than Ru, and when the B cation occupied period 6. The observed trend in activity was similar to that observed for the oxygen reduction reaction on transition metals, and was related to the strength of the bonding between the adsorbed oxygen species and the B-cation. The exceptional OER activity and stability of lead ruthenate pyrochlore catalysts were evaluated in a solid-state alkaline water electrolyzer. The overpotentials obtained were 0.1-0.2 V lower than for IrO_2 and the performance was stable for at least 200 h.

Introduction

Increasing energy demand and a drive towards clean energy has stimulated research activities directed towards new energy conversion and storage systems. Electrochemical devices such as fuel cells, water electrolyzers,[1] unitized fuel cells[2], rechargeable batteries[3] and redox flow batteries[4, 5] play a central part in many renewable/sustainable energy schemes. In most of these systems, there is increasing interest in the use of hydrogen as the fuel or energy vector.[6] Hence, water electrolysis technology plays an important role as a clean and efficient way to produce hydrogen. Solid-state alkaline water electrolyzers have recently attracted interest as an alternative to proton exchange membrane (PEM) water electrolyzers. [7-9] They offer an efficient, modular, and reliable method to produce hydrogen from water and renewable electricity sources.[10] The main benefit, in contrast with PEM electrolyzers, arises from the fact that the alkaline environment facilitates better oxygen evolution reaction (OER) kinetics and allows the use of a variety of stable OER catalysts, [1, 11-23] making it possible to reduce capital expenses. Given the high overpotentials associated with the OER, it is worthwhile to consider the issue of the development of efficient catalysts for the oxygen evolution reaction (OER) in alkaline media.[1, 24-27] In this study, we examine a variety of pyrochlore materials and evaluate their activity for the OER in alkaline media.

In recent work, Jin and coworkers investigated bifunctional catalysts for both HER and OER for applications in water splitting.[28] They synthesized cobalt oxide doped with nitrogen catalysts and evaluated their activity towards the HER and OER. They found a small onset potential (85 mV) for the HER using this material. Similarly, when used as catalysts for OER,

the cobalt oxide doped with nitrogen catalyst required only an overpotential of 0.26 V to obtain a current density of 10 mA cm^{-2}. The authors concluded that their results opened new possibilities for water splitting catalysts.

Pyrochlores are a diverse group of materials with disparate properties that facilitate their use in a number of applications. They are used as electrode materials, catalysts, resistors, magnetic materials, superconductors and capacitors.[29, 30] Subramanian and coworkers have extensively reviewed a large variety of pyrochlores in terms of their structure, properties and synthesis.[31] Pyrochlore compounds can be represented by the general formula $[A_2O'][B_2O_6]$, comprising a network of corner sharing BO_6 octahedra, with A and O' atoms occupying interstitial sites.[32] A scheme of the structure can be seen in **Fig S1** (Electronic Supplementary Information). Oxygen vacancies are usually formed preferentially at the interstitial O' sites rather than at the O sites. As a general rule, A is a lanthanide or non-metal, while B is a transition metal cation. When polarizable cations as Pb^{2+} and/or Bi^{3+} occupy the A site, the resulting pyrochlores have metallic conductivity. The metallic conductivity permits the preparation of self-supported electrodes for applications requiring large current densities simplifying membrane electrode assembly (MEA) fabrication and reducing Ohmic losses.

Horowitz and coworkers have shown that lead and bismuth ruthenate and iridate pyrochlores (with metallic conductivity) exhibit high activity towards the oxygen reduction reaction (ORR) in alkaline media. They also noticed that these pyrochlores exhibited activity for the OER in alkaline media. In their studies, the catalysts were prepared by precipitation/ crystallization in alkaline solutions at moderate temperatures. Low temperature synthesis yielded materials with relatively high surface areas (20-90m^2/g) that resulted in OER electrocatalytic activities of 5 Ag^{-1} at 1.3 V vs. RHE (at 75°C in 3M KOH). [33-41]

Pyrochlores containing ruthenate (RuO_4^{2-}) and iridate (IrO_3^{2-} and IrO_3^{-}) anions are not completely stable at high pH because they are slightly soluble in mild alkaline solutions.[42] Likewise, the dissolution of lead ($HPbO_2^{-}$ /PbO_3^{2-}) and bismuth (BiO_3^{-}) oxyanions in alkaline solutions is also a possibility, and has been suggested by several authors.[34, 35, 37, 43] However, this problem can be minimized or even solved by using anion exchange membranes instead of liquid alkaline solutions. Prakash and coworkers[34, 35] and Goodenough and coworkers[37, 43] proposed the use of solid ionomers (i.e. Nafion®) to protect the catalyst from direct attack from concentrated KOH solutions, and found that the pyrochlores were stable in this configuration. Alkaline ionomers (or anion exchange membranes) are not as basic as concentrated KOH solutions and the co-ion (quaternary ammonium) is fixed to the polymer backbone and so cannot participate in the solubilization of the ruthenate or iridate salts. This can help stabilize the pyrochlores, allowing stable OER catalysts.

In this work, we synthesized lead and/or bismuth ruthenate, iridate and osmate pyrochlores (the A cation was chosen to be Pb and/or Bi to get electronic conducting oxides) using wet chemistry and solid state methods. We measured their OER activity in alkaline medium using rotating disk electrode (RDE) experiments, by depositing a thin film catalyst layer on top of a glassy carbon electrode, to obtain accurate kinetic data. We compare their OER activity against a benchmark commercial OER catalyst (iridium oxide to evaluate their feasibility as OER catalysts for commercial applications in solid-state alkaline water electrolyzers. The electrocatalytic activity of pyrochlores and the mechanism for oxygen evolution are discussed and rationalized in terms of the electronic properties of the materials.

Experimental methods

Synthesis of $Pb_2Ru_2O_{6.5}$ and $Bi_{2.4}Ru_{1.6}O_7$ pyrochlores

Lead or bismuth ruthenate pyrochlores were synthetized following the alkaline solution technique first described by Horowitz and coworkers.[33] Ruthenium (III) chloride hydrate (5 mmol, $RuCl_3$, 35-40% Ruthenium, Acros) and lead acetate trihydrate (5 mmol, $Pb(C_2H_3O_2)_2$, 99%, Aldrich) were dissolved in approximately 50 mL DI water and stirred for 20 minutes. The mixture was precipitated in 500 mL 4M KOH, and the amorphous precipitate was crystallized by keeping it in the same KOH solution at 85°C with continuous oxygen bubbling for 5 days.[33] Then, the solid was recovered by centrifugation and washed with DI water until neutral wash water pH was reached, washed one time with glacial acetic acid (to remove any lead oxide impurities) and subsequently washed 5 times with acetone. Finally, the precipitate was dried using supercritical carbon dioxide (4,000 psi or 272 Atm and 45°C) to obtain a high surface area catalyst. In the case of lead ruthenate, this procedure resulted in a crystalline pyrochlore.

To prepare bismuth ruthenate pyrochlore ($Bi_{2.4}Ru_{1.6}O_7$), 6 mmol of $RuCl_3$ and 4 mmol of $Bi(NO_3)_3$ $5H_2O$ (Aldrich, 98%) were dissolved in 1M nitric acid and stirred for 20 minutes. The salt solution was precipitated in 500mL 0.1M KOH (O_2 saturated), the pH was adjusted to 13 (using 6M KOH), and the precipitate was kept in the liquid alkaline medium at 75°C, with continuous bubbling of pure oxygen for 7 days. The solid was recovered by centrifugation, washed with water and acetone and dried using supercritical carbon dioxide as described in previous paragraphs. The resulting catalyst was heat treated in argon atmosphere to get the crystalline pyrochlore (300°C for 24 hours and later at 500°C for another 24h).[33] The presence of crystalline pyrochlore phases was determined using XRD.[33, 44, 45]

Synthesis of $Pb_2Ir_2O_{6.5}$, $Bi_2Ir_2O_7$, $BiPbIr_2O_{6.5}$ and $Pb_2Os_2O_{6.5}$ pyrochlores

Lead and bismuth iridate and osmate pyrochlore catalysts were synthesized by solid state reaction.[45] A stoichiometric mixture of the oxides (PbO, IrO_2 and/or Bi_2O_3 in the case of iridate-based pyrochlores; and PbO and OsO_2 for the synthesis of osmate-based pyrochlores) was intimately mixed in a mortar

and heated in an alumina crucible at 800°C for 24 h. IrO_2 was obtained by heating $IrCl_3$ at 800°C in air for 1 h. The reaction was conducted in a tube furnace in argon atmosphere. The samples were periodically reground to get a good contact between the different oxides during heating. X-ray diffraction (XRD, Rigaku MiniFlex) revealed that all the products had a single-phase pyrochlore structure (**Fig. 1**).

Conductivity, XRD and B.E.T. surface area

The electronic conductivity of the pyrochlores was measured using a two-electrode conductivity cell designed and build in our laboratory, comprising two copper cylindrical electrodes inserted in a cylindrical polyether ether ketone block. Further details of the design and use of the conductivity cell can be found in our previous works.[46-48] The powdered sample was placed between the copper electrodes (0.32 cm^2), and compressed with the aid of 6 screws under a constant torque of 25 lb·in (0.29 kg·m). The sample thickness was determined by subtracting the thickness of the empty cell from the thickness of the assembled cell. The resistance (in ohms) was calculated using impedance spectroscopy and used to determine the conductivity (σ) of the pyrochlore:

$$\sigma = d/(R_{HF} \times A) \quad (1)$$

where σ is the conductivity, d the sample thickness, R_{HF}, the high frequency resistance, determined by the intercept of the impedance with the real axis, and A the electrode area. The resistance of the conductivity cell was approx. 0.1 mOhm, which can be considered sufficiently low to be neglected in the calculations.

X-ray diffraction (XRD) diffractograms were collected using a Rigaku Miniflex diffractometer. Diffractograms were recorded from 20° to 90° (2 theta, 2θ) at a rate of 0.5 degrees/min.

Catalyst surface area was determined from nitrogen absorption isotherms (B.E.T. surface area). The measurements were done multiple times for each sample using a QuantaChrome (QuantaSorb) instrument.

Measurement of OER activity

The method used to determine the electrochemical activity of the catalysts was an adaptation of the method developed by Suntivich and coworkers [49, 50] to determine the OER activity of metal oxides using RDE. Catalyst inks were prepared by ultrasonication (QSonica; Q700 sonicator) of 25 mg catalyst, 6mL of 24 vol% isopropanol/water, 0.275 mL of Nafion® solution (Aldrich; equivalent weight 1100, 5wt% solution in aliphatic alcohols) and 0.250mL of 1M KOH. KOH was added to neutralize the Nafion® binder, and avoid any corrosion of the oxide catalysts due to the strong acidity of Nafion®. The pyrochlores had electronic conductivities above 50 S/cm (see **Table 1**), and were tested without addition of any conductive support material because the ohmic losses in the electrodes were negligible.

10 μL of well-dispersed ink was deposited onto a freshly polished glassy carbon (GC) electrode (d=5mm; A=0.1964 cm^2) using a 10μL micropipette (Gilson). The GC was polished with 0.05μm alumina slurry (Pine Instruments) for 10 minutes until a mirror-like finish was obtained. The ink was dried using the technique described by Garsany and coworkers by rotating the RDE rotor in an inverted position.[51]
The rotation of the GC electrode during the drying precludes particle settling and/or aggregation, yielding high quality electrodes for electrochemical activity measurements. The catalyst loading was 200 μg-cm^{-2} disk.

Electrochemical experiments were carried out in an electrochemical cell using a three-electrode configuration. The GC electrode was attached to a rotator (Pine Instruments) to control the rotation rate, and the potential was controlled using a Solarton potentiostat (model 1480 multistat). All experiments were conducted at 5 mVs^{-1} in 0.1 M KOH electrolyte saturated with oxygen (Praxair, compressed gases, 4.0 grade) at room temperature. All the potentials in this work are referenced vs. the reversible hydrogen electrode (RHE). However, a saturated silver/silver chloride (Ag/AgCl) reference electrode was used in the experiments. A calibration of the Ag/AgCl electrode vs. RHE was done prior to the start of the experiments. The potential of the Ag/AgCl electrode was -0.973V vs. RHE. The applied potentials were IR corrected using the following equation:

$$E_{IR\,Corr} = E_{Appl} - IR \quad (2)$$

where I is the current and R is the ohmic resistance of the electrochemical cell, measured using impedance spectroscopy (Approx. 37 Ohm).

Oxygen evolution reaction (OER) activities were obtained from positive-going scans in O_2-saturated electrolyte (0.1M KOH) at 1600 rpm, and were corrected for capacitive currents. The current in the potential range 1.2-1.3 V vs. RHE was assumed to be only capacitive current. The activity for each catalyst was measured at least three times using newly prepared electrodes, and averaged. The error bars in the plots represent standard errors. The activities were calculated without any mass transport correction, assuming that the data was taken in the kinetic controlled region (since water is plentiful, it is unlikely that significant transport issues would exist). Experiments performed at different rotation rates did not show any significant differences between the currents measured, confirming the hypothesis.

Solid-state alkaline water electrolyzer

The catalyst performance and stability were also evaluated in a solid-state alkaline water electrolyzer. Electrolyzer experiments were performed in a modified 25cm^2 single cell (Fuel Cell Technologies Inc.) using ultrapure water unless specified (18.2 MΩ; Millipore Direct Q5 system). The anode graphite plate was replaced with a corrosion-resistant metal plate (with 1mm

x1mm single serpentine flow channels) to avoid carbon corrosion. The membrane electrode assemblies (MEAs) were prepared by sandwiching an anion exchange membrane (AEM, commercial 28μm thick membrane) between two gas diffusion electrodes (GDEs), each with an active area of 25 cm^2. Note: No heating or mechanical pressing was applied while sandwiching the AEM between the electrodes.

Gas diffusion electrodes (GDE) were prepared by painting (using an airbrush) the catalyst ink over a gas diffusion layer (GDL). We used two different GDLs: **1)** carbon paper (235 μm thick) for the cathode side, and **2)** porous corrosion-resistant metal substrate for the anode side. The catalyst ink consisted of 0.15 g catalyst, 3.2 g isopropanol/water (1/1 wt) and 1.286 g of 5wt% solubilized AEM binder. The mixture was sonicated for 10 minutes to get a homogeneous ink and was applied to the gas diffusion electrode using an airbrush. Platinum black (Sigma Aldrich, 10 m^2g^{-1}) was used as the hydrogen evolution (cathode) electrocatalyst, while iridium oxide (Proton OnSite) or the pyrochlore being evaluated was used as the oxygen evolution (anode) electrocatalyst. Electrodes with 3.0 $mgcm^{-2}$ of catalyst and 30wt% solubilized AEM binder were prepared in this work. The AEM and the electrodes were ion exchanged to the hydroxide form by immersion in 0.5M KOH overnight before electrolyzer testing. They were washed with abundant DI water and assembled quickly before testing, in a nitrogen environment within a glovebag (Sigma Aldrich), to minimize exposure to atmospheric carbon dioxide.

Ultrapure water was fed to the anode and recirculated to a storage tank, which was maintained at 50°C, at a flow rate of approximately 400 $mLmin^{-1}$. The absence of water feed at the cathode facilitates the recovery of dry hydrogen.

Polarization curves were obtained at 50°C by stepping the current density from 100 $mAcm^{-2}$ to 1000 $mAcm^{-2}$ in increments of 100 $mAcm^{-2}$. The system was held at each current density for 2 minutes to allow pseudostationary conditions. The acquisition was stopped when the voltage increased above 2.2 V.

Results and discussion

Characterization of the catalyst: X-Ray diffraction (XRD), B.E.T surface area and electronic conductivity.

X-ray diffractograms (**Fig. 1**) were used to confirm the presence of pyrochlore phases and to obtain a quantitative estimate of their lattice parameters. The peaks associated with $Pb_2Ru_2O_{6.5}$ pyrochlore were seen at 2θ values of 30°, 35°, 50°, 59, 62°, 73°, 81° and 84° representing the (222), (400), (440), (622), (444), (800), (662) and (840) Bragg's reflections of the cubic (space group: Fd-3m) structure of pyrochlore. The position of the XRD peaks changed slightly for the other pyrochlores as a consequence of changes in lattice parameters.

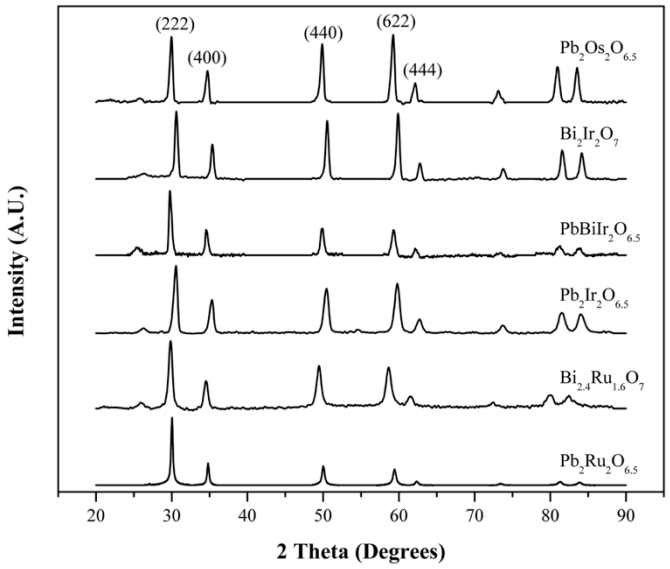

Figure 1. X-ray diffractograms of lead and bismuth ruthenate, lead and bismuth iridate and lead osmate pyrochlores.

The reduction of unit cell dimensions is manifested as an XRD peak shift to higher angles. [45] The smallest unit cell corresponded to $Pb_2Ir_2O_{6.5}$, and the largest to $Bi_{2.4}Ru_{1.6}O_{7-y}$ (see **Table 1**). The lattice parameters for lead and bismuth pyrochlores were in good agreement with the values reported by Horowitz and coworkers.[41] The substitution of Ru by Bi (larger cation) in the octahedral B site position ($Bi_{2.4}Ru_{1.6}O_{7-y}$) leads to enlargement of the cubic unit cell volume as previously reported.[33] $BiPbIr_2O_{6.5}$ lattice parameters were also in good agreement with the data reported by Kennedy,[45] but the lattice parameters calculated in this work for $Pb_2Ir_2O_{6.5}$ and $Bi_2Ir_2O_7$ were approximately 0.02 nm lower than literature values.[45]

TEM analysis showed that the lead ruthenate pyrochlore comprised particle-like aggregates of approximately 50-100 nm, which themselves were made up of smaller particles glued together (See **Fig. S2**). HRTEM also revealed (as expected) that some particles were crystalline.

Table 1. Properties of the pyrochlore OER electrocatalysts

Catalyst	Unit cell dimensions* a=b=c (Å)	Unit cell volume ($Å^3$)	Calculated density (g/cm^3)	B.E.T. surface area (m^2/g)	Electronic conductivity S/cm
$Pb_2Ru_2O_{6.5}$	10.34(9)	1108	8.64	99±4	120±30
$Bi_{2.4}Ru_{1.6}O_7$	10.44(4)	1139	9.04	7.8±0.2	63±5
$Pb_2Ir_2O_{6.5}$	10.07(6)	1023	11.73	1.2±0.1	73±7
$Bi_2Ir_2O_7$	10.11(4)	1035	11.74	0.4±0.1	56±6
$BiPbIr_2O_{6.5}$	10.31(7)	1098	10.94	0.4±0.1	75±7
$Pb_2Os_2O_{6.5}$	10.36(2)	1112	10.73	0.8±0.3	53±7

* cell type: cubic: a=b=g=90°, a=b=c; space group: Fd-3m; 8 molecules in the unit cell.

The pyrochlores exhibited conductivities above 50 S/cm (metallic conductivity) with lead ruthenate having the largest conductivity (See Table 1). These conductivities were for the materials in powder form, which usually underestimate the value of the conductivity (the air inside the pores does not conduct), and were measured using a two-electrode conductivity cell. For a hypothetical electrode with a thickness of 50 μm, the electrode electronic resistance will be less than 0.1 mOhm-cm^2, well below permissible limits for high performance in a device.

The BET surface areas for the lead ruthenate pyrochlore were around 100 m^2/g whereas specific surface areas for bismuth ruthenate, and lead and bismuth iridates and osmates ranged 0.4-8 m^2/g. This result was a consequence of heating treatment employed during the synthesis of pyrochlores other than the lead ruthenate pyrochlore to enhance crystallinity, as described in the experimental section.

OER activity

Lead ruthenate and bismuth ruthenate pyrochlores had previously been identified as highly active catalysts for the ORR in alkaline media by several authors.[33-35, 37] Their exceptional ORR activity amongst metal oxides arises from their relatively high electronic conductivity, surface area, and their electronic properties.[52-55] As confirmed here, their OER activity is even more exceptional, outperforming other mixed oxides and even commercial state of the art catalysts for water electrolysis. **Fig. 2** compares the OER activity (half-cell polarization curves in RDE electrode) for the five pyrochlores examined in this work, showing the background corrected current density vs. IR corrected potential at 1,600 rpm. Pt black and IrO_2 benchmark are also included in the graph for comparison purposes. The lead ruthenate pyrochlore displayed an OER onset potential as low as 1.4 V (vs. RHE) and OER current densities as high as 40 mAcm^{-2} disk, despite the low catalyst loadings. In most of the works reported in the literature, the catalyst loadings were in the interval 6-60 mgcm^{-2},.[33, 35] Herein, we decided to prepare electrodes with catalyst loadings between 100 to 200 μg/cm^2 disk to minimize the mass transport losses within the electrode, and to get more accurate kinetic currents, less influenced by mass transfer and/or cell resistance losses.[50]. The background contributions from the glassy carbon (GC) electrode can be considered insignificant since the OER on GC substrate was very low even at 1.9 V vs. RHE (see baseline in **Fig. 2**), and because the catalyst deposited onto the GC electrode covers it completely (see **Fig. S5**). The oxygen bubbling on the surface of the electrode was very intense during the experiment, and was used as a direct confirmation that the measured current was due to OER.

The OER activity was calculated from polarization curves taken at a rotation rate of 1,600 rpm to minimize mass transport losses as a consequence of bubbles present in the surface of the electrode.

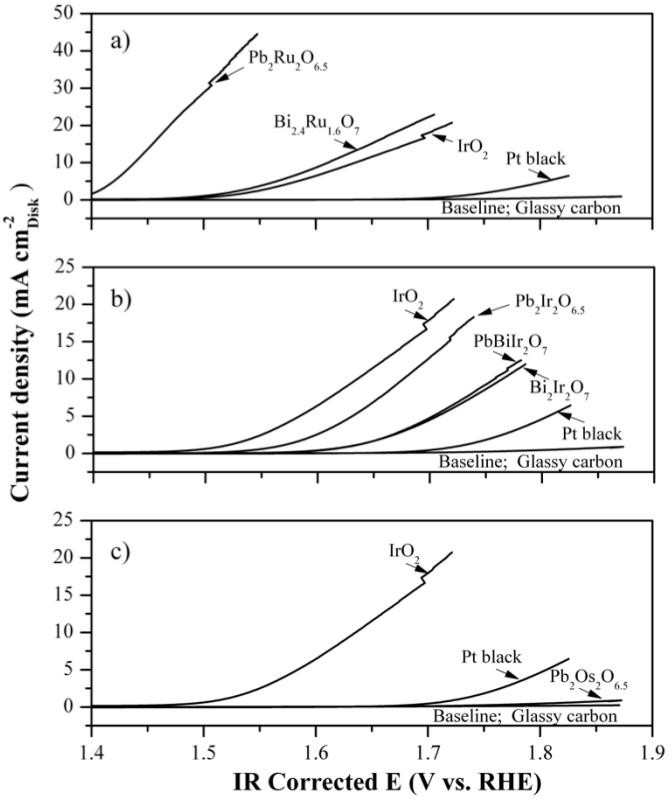

Figure 2. OER polarization curves for a) lead and bismuth ruthenate pyrochlores ($Pb_2Ru_2O_{6.5}$, $Bi_{2.4}Ru_{1.6}O_7$), b) lead and bismuth iridate pyrochlores ($Pb_2Ir_2O_{6.5}$, $Bi_2Ir_2O_7$, $PbBiIr_2O_{6.5}$) and lead osmate pyrochores ($Pb_2Os_2O_{6.5}$) in 0.1 M KOH at room temperature. IrO_2 and Pt black were used for comparison purposes. IR correction of the potential was done from capacitance-corrected positive-going scans at 5 mV s^{-1} using high frequency cell resistance measured by impedance spectroscopy. Catalyst loadings were approx. 200μg/cm^2. Glassy carbon area was 0.196 cm^2.

Capacitance corrected currents and the catalyst loading in the electrode were used to calculate mass activities (**Fig. 3**) The low loadings of the catalyst allowed a good estimate of mass activity. The OER activity for $Pb_2Ru_2O_{6.5}$ calculated from the data of Horowitz and coworkers[33] (the catalyst loading was 60mg/cm^2, and the experiment was done in 3M KOH at 75^{o}C) was ~5A/g at 1.4V (vs. RHE), which was considerable lower than our results for the same catalyst (35 A/g at 1.4V vs RHE). From the data of Prakash and coworkers[35] we estimated an OER activity for $Pb_2Ru_2O_{6.5}$ between 0.1-0.5 A/g (at 1.3V-1.5V), which was also considerably lower than the results obtained in this work.

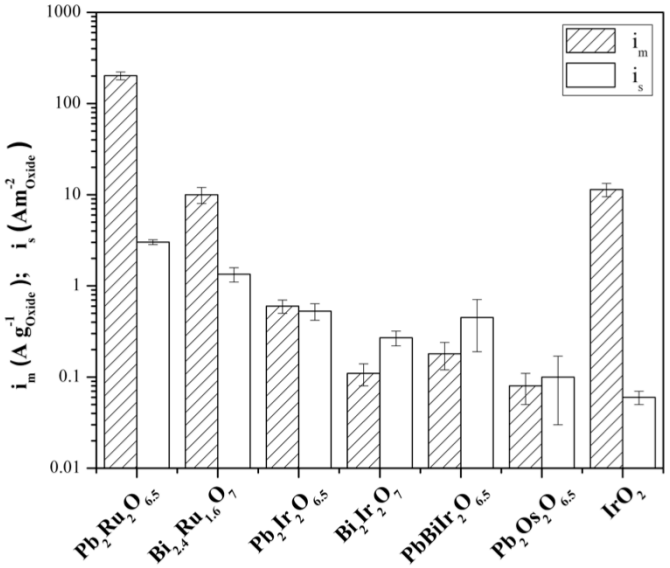

Figure 3. OER mass (i_m) and specific (i_s) activities for $Pb_2Ru_2O_{6.5}$, $Bi_{2.4}Ru_{1.6}O_{6.9}$, $Pb_2Ir_2O_{6.5}$, $Bi_2Ir_2O_7$, $PbBiIr_2O_{6.5}$, $Pb_2Os_2O_{6.5}$, IrO_2 and Pt black. Activities were measured at 1.5 V vs RHE (IR corrected potential). Error bars represent standard deviations from at least three independently repeated measurements.

The OER activity of IrO_2 (state-of-the-art catalyst used in commercial PEM electrolyzers) was also measured using the thin film method. The activity was 11±2 A/g (at 1.5 V vs. RHE), slightly higher than previously reported OER activities. Suntivich and coworkers reported an OER activity for IrO_2 of 7 A/g (at 1.5 V vs. RHE), but their catalyst had a surface area of 71 m^2/g whereas the catalyst tested in this work had a surface area of 185 m^2/g.[56] The OER activity was also calculated per gram of platinum group metal (PGM) and normalized based on the price of PGM to show the exceptional activity of ruthenate based OER catalysts, and its suitability for commercial applications (see **Figs. S3 & S4**). The activity of lead ruthenate pyrochlore OER catalyst (based on PGM content or PGM price) was 3-4 orders of magnitude higher than that of the state-of-the-art iridium oxide OER electrocatalyst.

The catalysts evaluated in this work had varying surface areas as a consequence of differences in the synthesis methods used to prepare the crystalline materials (See **Table 1**), making the comparison of the mass activities difficult. Lead and bismuth iridate and osmate pyrochlores required several heating cycles to obtain crystalline phases. The reaction rates in heterogeneous catalysts are commonly expressed as surface area–normalized rates (specific activity, i_s) to remove the surface area dependence and to allow a proper comparison of the intrinsic catalytic activities. The specific activity (OER current per catalyst surface area) offers a means to compare catalysts with varying surface areas since OER is a heterogeneous reaction occurring at the surface of the catalyst, and the reaction rate depends on the total amount of surface active sites available. **Fig. 3** shows the specific-surface activity (mass activity divided by the catalyst BET surface area) for the pyrochlores. Lead ruthenate pyrochlore had the highest specific activity (3.0 Am^{-2}), followed by bismuth ruthenate pyrochlore at approximately 2-fold lower), and the iridate-based pyrochlores that had specific activities 6-10 times lower than that of lead ruthenate pyrochore. IrO_2 had a surface-specific activity of 0.06 Am^{-2}, which was 50 times lower than that of lead ruthenate. Our measurements for IrO_2 consistently yielded a slightly higher surface-specific OER activity than those found in previous reports (0.04 Am^{-2}).[56] We attribute it to the ability of our method and the conditions used (catalyst loading, film thickness, rotation rate, etc.) to measure the true kinetic currents during RDE experiments.

Given these experimental results, we attempted to rationalize and better understand the trends seen. Suntivich and coworkers[49, 50, 56] proposed the filling of e_g antibonding orbitals as an activity descriptor for OER and ORR in perovskite catalysts. They hypothesized that the antibonding orbital (e_g) occupation influences the strength of the bond between the B cation and oxygen species involved as intermediates in the OER.. The metal in the active center that they studied was one among Co, Mn, Fe, Cr or Ni (4th period, 3d electrons) and they found a typical volcano-type dependence for the activity vs. the filling of antibonding orbitals. In octahedrally coordinated species, as in the case of B cation in perovskites and pyrochlores, there are three bonding orbitals (t_{2g}) and two antibonding orbitals (e_g) resulting from the octahedral crystal field splitting of the d orbitals. Suntivich and co-workers found that the maximum activity corresponded to an e_g filling near 1.2. The reaction mechanism proposed by Suntivich and co-workers involves the formation of several oxygen intermediates bonded to the B site in the mixed oxide catalyst (perovskite or pyrochlore), and the intermediate filling of the antibonding e_g orbitals represents an intermediate bonding energy for the oxygen species. More electrons in the antibonding orbitals (e_g) leads to destabilization of the complex, and a weaker bond between the oxygen intermediates and the B cation. If the bond is weak, the oxidation of the intermediates proceeds at lower rates because they can desorb from the active site before they are completely oxidized to O_2. This reaction mechanism is a well-known and generally accepted mechanism for OER in metal oxides (See **Fig. 4**). [43, 56] Indirect confirmation that the B cation is responsible for OER activity was found in experiments performed with pyrochlores prepared with partial substitution of the B cation. In a series of experiments, we synthesized lead rich ruthenium pyrochlores ($Pb_2Ru_2O_{6.5}$, $Pb_{2.3}Ru_{1.7}O_{6.5}$, $Pb_{2.5}Ru_{1.5}O_{6.5}$, $Pb_{2.7}Ru_{1.3}O_{6.5}$, and $Pb_{2.9}Ru_{1.1}O_{6.5}$) and evaluated their OER activity. The specific OER activity decreased for pyrochlores with lower Ru content, evidencing that Ru was the active element in the catalyst (see **Fig. S6**).

To investigate the validity of the same activity descriptor (e_g antibonding orbital filling) for pyrochlore based catalysts, we calculated the filling of antibonding orbitals for the ruthenate and iridate based pyrochlores. The 4d and 5d orbitals are more extended compared to 3d orbitals, and hence hybridization of the transition metal d orbitals and oxygen 2p orbitals is much more pronounced than the d-d orbital interactions, resulting in

an increase of octahedral crystal field splitting. In general, for octahedral complexes with strong field ligands or 4d/5d transition metals (Ru and Ir are 4d and 5d respectively) there is a large octahedral crystal field splitting energy, and the electronic configuration is always low spin (filling of lower energy orbitals occurs first). The oxidation state of Ru and Ir in the pyrochlores was between 3.6^+ and 5^+ resulting in empty antibonding orbitals (e_g) for all the cases (See ESI for details of the calculations). Since the activity of the pyrochlores was greater than those of the perovskites (from literature), it is clear that this descriptor was not sufficient to describe the trends in activity. This result suggested that other electronic properties of the catalyst affect the bond strength between the B site and the intermediate oxygen species.

Rossmeisl and coworkers demonstrated using DFT calculations that the binding energies of HO, O and HOO on metal oxide surfaces (IrO_2, RuO_2 and TiO_2) are linearly correlated, and can be used to predict OER activity on metal oxide surfaces. They found that the activity had a maximum for RuO_2, which had an adsorbate bonding energy that was just appropriate; not too strong that the oxygen could not desorb after the oxidation steps; not too weak that the intermediates desorbed before the final product is formed. Hammer and Nørskov[57] showed that the binding energies (obtained DFT calculations) for oxygen and transition metals change along the periodic table following two general trends: **1)** the farther to the left in the periodic table, the stronger the bond; and **2)** the farther down in the periodic table, the weaker the interaction. As we move to the left side of the periodic table, the d bands move up in energy (see **Table S1**) and more antibonding adsorbate-transition metal states become empty, resulting in a stronger bond between the metal and the adsorbate. The second effect arises from the interaction between the oxygen 2p orbitals (it can also be applied to oxygen intermediates or other adsorbates in the general case) and transition metal (B-site) d orbitals. The repulsive interaction raises the energy by an amount that is proportional to the square of the adsorbate–metal *d* coupling matrix element (V^2, tabulated in **Table S1**). The stronger the overlap, the larger the repulsion (the larger V^2_{ad}), and the weaker the bond between the intermediate oxygen species and the transition metal (B= Ru, Ir or Os).

To test if these rules applied here, we compared OER activity of lead and bismuth ruthenate, iridate and osmate pyrochlores.[31, 58-60] Osmium (Xe $4f^{14}$ $5d^6$ $6s^2$) is below ruthenium in the periodic table (Kr $4d^7$ $5s^1$), but belongs to the same group so it is expected to have lower binding energies for oxygen intermediates than ruthenate-based pyrochores, and therefore lower OER activity than ruthenate-based pyrochlores, as we found experimentally. The catalyst had a mass activity (at 1.5 V vs. RHE) of 0.08±0.03 A/g and a surface activity of 0.1±0.05 A/m^2 (See **Fig. 3**).

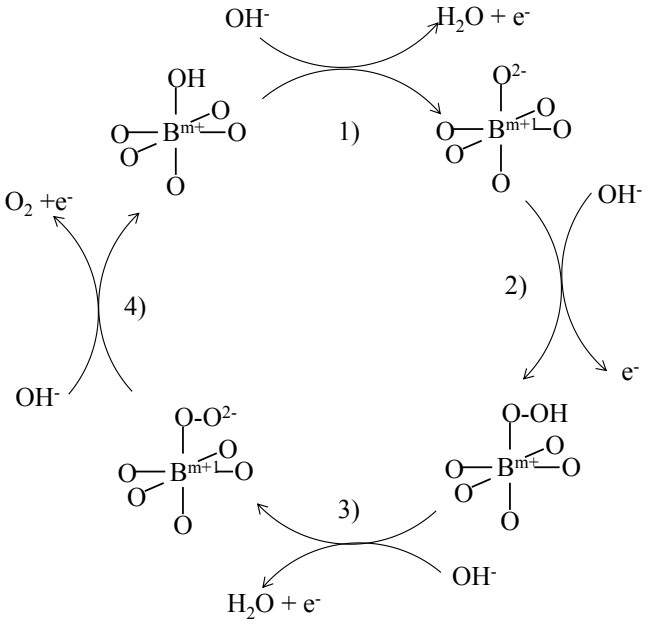

Figure 4. Proposed reaction mechanism for the OER on pyrochlore electrocatalyst. The scheme is similar to the mechanisms proposed by Goodenough and coworkers,[37] and by Suntivich and coworkers[56] for OER in metal oxides. The reaction proceeds via 4-electron transfer steps, and the rate limiting steps are the O-O bond formation (2) and the proton removal of the oxyhydroxide group (3).

Iridium has smaller adsorbate (*s* or *p*)–metal *d*-coupling matrix element (V^2_{ad}) than osmium (See **Table S1** in the ESI) and hence the repulsion between the d orbitals of transition metal and 2p orbitals of oxygen raises less than the energy of the d orbitals and results in a stronger bond between oxygen and the B metal. The binding energy between the oxygen and ruthenium is more close to iridium than osmium and hence the OER activity of iridate-based pyrochlores should be more close to those of ruthenate-based pyrochlores than osmate-based pyrochlores. The experimental results corroborate these predictions (see specific-surface activities in **Fig. 3** and table S1). The specific-activity of iridate-based pyrochlores was between 0.3-0.5 A/m^2, lower than ruthenate-based pyrochlores (3.0-1.3 A/m^2) but slightly higher than for osmate-based pyrochlores (~0.1 A/m^2). (Note: the activities were calculated at a potential of 1.5 V vs. RHE).

Evaluation of the OER catalyst performance in a solid-state alkaline water electrolyzer

The polarization curves obtained for MEAs fabricated with $Pb_2Ru_2O_{6.5}$, $Bi_{2.4}Ru_{1.6}O_7$ and IrO_2 catalysts (OER) are shown in **Fig 5**. The electrolyzer was operated with ultrapure water (18.2 MΩ-cm). The alkaline conditions result from the presence of the alkaline membrane (AEM) and solubilized AEM binder in the electrodes (there was no addition of free base).

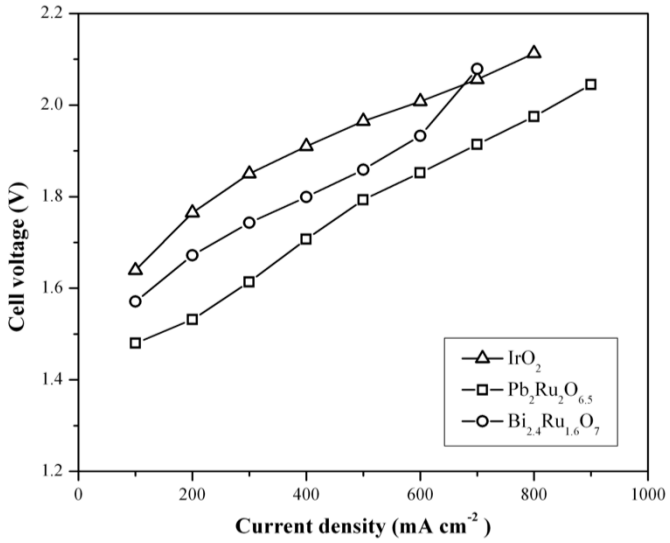

Figure 5. Electrolyzer polarization curves (at 50°C) for MEAs prepared with $Pb_2Ru_2O_{6.5}$, $Bi_{2.4}Ru_{1.6}O_7$ and IrO_2 OER catalysts. Platinum black was used as hydrogen evolution catalyst (HER). Catalyst loadings were 3.0 mgcm^{-2}.

The MEAs were prepared with a commercial AEM and binder, and the catalyst loading for both the anode (pyrochlore or iridium oxide) and cathode (platinum black) was 3.0 mg-cm^{-2}. The lead ruthenate MEAs exhibited 0.1-0.15 mV lower overpotential than the MEAs fabricated with IrO_2 as the anode catalyst. This result confirms the exceptional OER activity of lead ruthenate pyrochlores ascertained via RDE experiments. The performance of the anion exchange membrane water electrolyzer was similar to performances reported by Hickner and co-workers[61] and Xiao and coworkers[62], with their own membranes, where current densities of 400 mA cm^{-2} at 1.8 V were achieved.

Additionally, the water electrolyzer performance in this work exceeded the performance by Faraj and coworkers where the authors used a radiation grafted low-density polyethylene AEM containing a quaternary ammonium group with a potassium carbonate doped water feed to boost system ionic conductivity, and to provide pH buffering (around 10).[63] Nevertheless, the performance reported herein is significantly lower than the performance of state-of-the–art PEM electrolyzers, which can be operated at 1.9 V at current densities as high as 1800 mA cm^{-2}.[7, 8] The main reasons for the gap in performance are larger polarization losses at the cathode (hydrogen evolution reaction is more sluggish in alkaline media) and the significantly lower ionic conductivity of the AEM compared to commercially available proton exchange membranes.[64]

Stability of OER catalyst during operation in a solid-state alkaline water electrolyzer

The stability of the catalysts was evaluated during continuous operation in the electrolyzer at 200 mA cm^{-2} for 200 h. **Fig. 6** shows a comparison of the stability of MEAs prepared with lead ruthenate and iridium oxide. We used iridium oxide in the comparison because it is well known from studies with PEM electrolyzers and also from commercial applications that iridium oxide is a very stable OER catalyst. The electrolyte employed was 1% $KHCO_3$ (in water) instead of ultrapure water and the temperature of the experiment was 35°C. Other experimental conditions similar to those used to obtain the polarization curves (see previous section and experimental section). We added 1% $KHCO_3$ to the water to enhance the ionic conductivity in the electrodes and minimize the effect of AEM binder loss / degradation on the overall performance.

Minimizing those losses will allow a better comparison of the stability of the electrocatalyst during operation of the solid-state water electrolyzer for an extended time period. We already know from previous work that the MEA performance degrades quickly when operated with ultrapure water.[65, 66] The performance degradation in these studies was located mainly on the anode side, and arose from the degradation of the AEM binder. By including a salt in the electrolyte, we can operate the electrolyzer at relatively low overpotentials without relying on the solubilized AEM binder for ionic transport in the electrodes.

The solid-state water electrolyzer prepared with lead ruthenate pyrochlore electrocatalyst showed stable operation for at least 200 h (see **Fig. 6**). The cell voltage increased slightly during the first 100 hours (~20 mV) but later remained almost constant at 1.75 V. The MEA fabricated with iridium oxide was also stable for the same period of time, but the operating voltage (as expected from the lower activity shown in **Figs. 2&3**) was 0.1-0.15 V higher at the same current density. Polarization curves and stability experiments confirmed the exceptional activity and stability of lead ruthenate pyrochlore as OER catalyst for solid-state alkaline water electrolyzers.

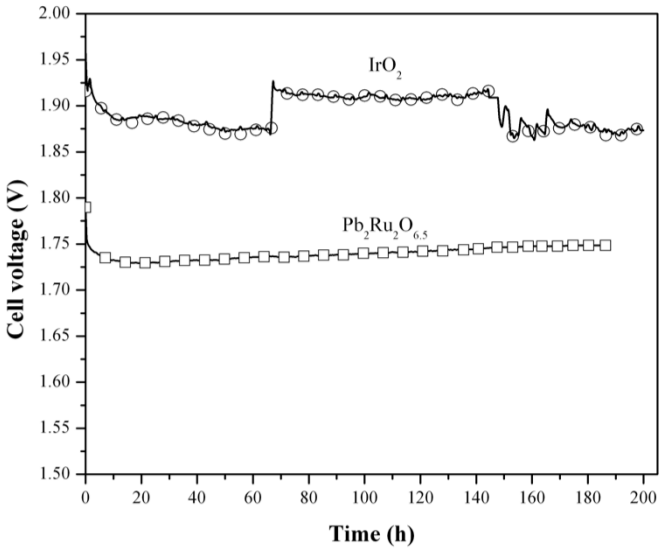

Figure 6. Durability of lead ruthenate pyrochlore during operation of a solid-state alkaline water electrolyzer at 200 mAcm^{-2}. The electrolyte was 1%$KHCO_3$ (in water) and the temperature was approx. 35°C. Cathode catalyst was Pt black (3.0 mgcm^{-2}), and anode catalyst were lead ruthenate pyrochlore or iridium oxide (3.0 mgcm^{-2}).

Conclusions

In this work we synthesized a series of electrically conducting metal oxides with the pyrochlore structure ($A_2B_2O_{7-y}$, with A=Pb or Bi and B= Ru, Ir or Os). The synthesis methods included precipitation/crystallization in alkaline medium for the synthesis of lead and bismuth ruthenates, and solid-state reaction for the synthesis of lead and/or bismuth iridates and osmates. The methods were chosen to achieve well-crystallized oxides with pyrochlore structure. The electrocatalytic activity of the catalysts for the oxygen evolution reaction (OER) in alkaline medium was studied using an RDE in 0.1M KOH. Lead and bismuth ruthenate pyrochlores showed significantly lower overpotentials for the OER than state-of-the-art IrO_2 catalysts. Mass activities (at 1.5 V vs. RHE) of 202±20 Ag^{-1}, 10±2 Ag^{-1} and 11±2 Ag^{-1} were found for $Pb_2Ru2O_{6.5}$, $Bi_{2.4}Ru_{1.6}O_7$, and IrO_2 respectively. Specific activities (at 1.5 V vs. RHE) of 3.0±0.2 Am^{-2}, 1.3±0.2 Am^{-2} and 0.06±0.01 Am^{-2} were determined for $Pb_2Ru_2O_{6.5}$, $Bi_{2.4}Ru_{1.6}O_7$, and IrO_2.

Lead and bismuth iridate and osmate pyrochlores were also synthesized and evaluated as OER catalysts. Mass activities for iridate-based catalyst were in the interval 0.1-0.6 Ag^{-1}. Very low B.E.T. surface areas (~1 m^2g^{-1}) and relatively low specific activities contributed to the low mass activities of iridate-based pyrochlores. Specific activities for iridate-based pyrochlores (0.3-0.5 Am^{-2}) were 5-10 times lower than for lead ruthenate pyrochlores. Lead osmate showed the lowest OER activity among all the pyrochlores, with mass and specific activities of 0.08±0.03 Ag^{-1} and 0.10±0.07 Am^{-2}.

We proposed that the reaction path for the OER involved several oxygen intermediate species (-O^{2-}, -OOH, -OO^{2-}, -OH) bonded to the B-cation in the pyrochlore, and that the catalytic activity depended on the bonding strength between the B-cation site (Ru, Ir or Os) and the oxygen species. This hypothesis is supported by the fact that OER activity correlated with Ru concentration in lead ruthenate pyrochlores prepared with varying amounts of Ru. The specific OER activity showed dependence on the occupancy of the 3d orbitals (group) and on the period in the periodic table occupied by the B-cation. The maximum specific activity was found for ruthenate-based pyrochlores, and was explained by an optimum interaction between oxygen intermediates and B-metal that results in a bond of the appropriate strength. The OER activity decreased for pyrochlores with B cations having more d electrons than Ru, and when the B cation occupied period 6.

The OER activity can be rationalized using the electronic properties of the corresponding B metal of the pyrochlore: **1)** d bands' center energy and **2)** square of the adsorbate–metal d coupling matrix element. As the d bands shift up in energy, the antibonding orbitals become depopulated, resulting in a stronger bond. Similarly, the interaction between the metal d electrons and the oxygen 2p states raises the energy by an amount that is approximately proportional to the square of the adsorbate–metal d coupling matrix element; the stronger the overlap, the larger the repulsion, and the weaker the bond between the oxygen intermediates and the transition metal.

Lead and bismuth ruthenate pyrochlore catalysts were tested in a solid-state alkaline water electrolyzer. The overpotentials were 0.1-0.2 V lower than for IrO_2 and the performance was stable was for at least 200 h.

Acknowledgements

We would like to thank the Department of Energy Small Business Innovative Research (SBIR) program, phases I and II (grant number DE-SC0007574) for funding this work.

Notes and references.

[a] Center for Electrochemical Science and Engineering, Department of Chemical and Biological Engineering, Illinois Institute of Technology, 10 W. 33rd St., Chicago, IL 60616, USA
*Corresponding author's e-mail: ramani@iit.edu

[b] Proton Energy Systems, Wallingford, CT 06492, USA

† Electronic Supplementary Information (ESI) available: [details of any supplementary information available should be included here]. See DOI: 10.1039/b000000x/

1. K. Zeng and D. Zhang, *Progr. Energy Combust. Sci.*, 2010, **36**, 307-326.
2. J. Pettersson, B. Ramsey and D. Harrison, *J. Power Sources*, 2006, **157**, 28-34.
3. H. Zhou, Y. Wang, H. Li and P. He, *ChemSusChem*, 2010, **3**, 1009-1019.
4. R. Zaffou, W. N. Li and M. L. Perry, *ACS Symp. Ser.*, 2012, **1096**, 107-127.
5. A. Z. Weber, M. M. Mench, J. P. Meyers, P. N. Ross, J. T. Gostick and Q. Liu, *J. Appl. Electrochem.*, 2011, **41**, 1137-1164.
6. N. Armaroli and V. Balzani, *ChemSusChem*, 2011, **4**, 21-36.
7. K. E. Ayers, E. B. Anderson, C. B. Capuano, B. D. Carter, L. T. Dalton, G. Hanlon, J. Manco and M. Niedzwiecki, *ECS Trans.*, 2010, **33**, 3-15.
8. K. E. Ayers, C. B. Capuano and E. B. Anderson, *ECS Trans.*, 2012, **41**, 15-22.
9. Y. Zhang, C. Wang, N. Wan, Z. Liu and Z. Mao, *Electrochem. Commun.*, 2007, **9**, 667-670.
10. E. Guerrini and S. Trasatii, eds. P. Barbaro and C. Bianchini, Wiley-VCH, Weinheim, 2009.
11. G. Schiller, R. Henne, P. Mohr and V. Peinecke, *Int. J. Hydrogen Energy*, 1998, **23**, 761-765.
12. Y. W. D. Chen and R. N. Noufi, *J. Electrochem. Soc.*, 1984, **131**, 1447-1451.
13. A. J. Esswein, M. J. McMurdo, P. N. Ross, A. T. Bell and T. D. Tilley, *J. Phys. Chem. C*, 2009, **113**, 15068–15072.
14. D. E. Hall, *J. Electrochem. Soc.*, 1981, **128**, 740-746.
15. D. E. Hall, *J. Electrochem. Soc.*, 1985, **132**, 41C-48C.
16. M. Hamdani, M. I. S. Pereira, J. Douch, A. Ait Addi, Y. Berghoute and M. H. Mendonça, *Electrochim. Acta*, 2004, **49**, 1555-1563.
17. J. Y. Huot, M. L. Trudeau and R. Schulz, *J. Electrochem. Soc.*, 1991, **138**, 1316-1321.

18. F. Rosalbino, D. Macciò, E. Angelini, A. Saccone and S. Delfino, *J. Alloys Compd.*, 2005, **403**, 275-282.
19. R. N. Singh, L. Bahadur, J. P. Pandey, S. P. Singh, P. Chartier and G. Poillerat, *J. Appl. Electrochem.*, 1994, **24**, 149-156.
20. R. N. Singh, A. N. Jain, S. K. Tiwari, G. Poillerat and P. Chartier, *J. Appl. Electrochem.*, 1995, **25**, 1133-1138.
21. R. N. Singh, S. K. Tiwari, S. P. Singh, N. K. Singh, G. Poillerat and P. Chartier, *J. Chem. Soc., Faraday Trans.*, 1996, **92**, 2593-2597.
22. H. Michishita, Y. Misumi, D. Haruta, T. Masaki, N. Yamamoto, H. Matsumoto and T. Ishihara, *J. Electrochem. Soc.*, 2008, **155**, B969.
23. C. Fan, D. L. Piron, A. Sleb and P. Paradis, *J. Electrochem. Soc.*, 1994, **141**, 382-387.
24. M. Wang and L. Sun, *ChemSusChem*, 2010, **3**, 551-554.
25. N. H. Chou, P. N. Ross, A. T. Bell and T. D. Tilley, *ChemSusChem*, 2011, **4**, 1566-1569.
26. S. Park, Y. Shao, J. Liu and Y. Wang, *Energy & Environmental Science*, 2012, **5**, 9331-9344.
27. H. Dau, C. Limberg, T. Reier, M. Risch, S. Roggan and P. Strasser, *ChemCatChem*, 2010, **2**, 724-761.
28. H. Jin, J. Wang, D. Su, Z. Wei, Z. Pang and Y. Wang, *J. Am. Chem. Soc.*, 2015, **137**, 2688-2694.
29. S. Trasatti, *Electrodes of Conductive Metallic Oxides*, Elsevier, 1980.
30. N. P. Raju, E. Gmelin and R. K. Kremer, *Phys. Rev. B: Condens. Matter*, 1992, **46**, 5405-5411.
31. M. A. Subramanian, G. Aravamudan and G. V. S. Rao, *Prog. Solid State Chem.*, 1983, **15**, 55-143.
32. R. A. McCauley, *J. Appl. Phys.*, 1980, **51**, 290-294.
33. H. S. Horowitz, J. M. Longo, H. H. Horowitz and J. T. Lewandowski, *ACS Symp. Ser.*, 1985, **279**, 143-163.
34. J. Prakash, D. Tryk and E. Yeager, *J. Power Sources*, 1990, **29**, 413-422.
35. J. Prakash, D. A. Tryk and E. B. Yeager, *J. Electrochem. Soc.*, 1999, **146**, 4145-4151.
36. M. Sansernnivet and P. Limthongkul, *Songklanakarin J. Sci. Technol.*, 2009, **31**, 669-673.
37. J.-M. Zen, R. Manoharan and J. B. Goodenough, *J. Appl. Electrochem.*, 1992, **22**, 140-150.
38. H. S. Horowitz, J. T. Lewandowski and J. M. Longo, Exxon Research and Engineering Co., USA . 1980, pp. 9 pp. Cont.-in-part of U.S. 4,129,525.
39. H. S. Horowitz, J. M. Longo and J. T. Lewandowski, Exxon Research and Engineering Co., USA . 1978, p. 13 pp.
40. H. S. Horowitz, J. M. Longo and J. T. Lewandowski, Exxon Research and Engineering Co., USA . 1979, pp. 7 pp. Cont.-in-part of U.S. 4,129,525.
41. H. S. Horowitz, J. M. Longo and J. T. Lewandowski, *Materials Research Bulletin*, 1981, **16**, 489-496.
42. M. Pourbaix, *Atlas of electrochemical equilibria in aqueous solutions*, National Association of Corrosion Engineers, Houston, Texas, 1974.
43. J. B. Goodenough and R. Manoharan, *Proc. - Electrochem. Soc.*, 1992, **92-11**, 523-539.
44. G. Gulsun and B. J. Kennedy, *J. Electroanal. Chem.*, 1994, **368**, 235-239.
45. B. J. Kennedy, *Physica B*, 1998, **241-243**, 303-310.
46. C.-P. Lo, G. Wang, A. Kumar and V. Ramani, *Appl. Catal., B*, 2013, **140-141**, 133-140.
47. A. Kumar and V. Ramani, *J. Electrochem. Soc.*, 2013, **160**, F1207-F1215.
48. A. Kumar and V. Ramani, *Appl. Catal., B*, 2013, **138-139**, 43-50.
49. J. Suntivich, H. A. Gasteiger, N. Yabuuchi, H. Nakanishi, J. B. Goodenough and Y. Shao-Horn, *Nat. Chem.*, 2011, **3**, 546-550.
50. J. Suntivich, H. A. Gasteiger, N. Yabuuchi and S.-H. Yang, *J. Electrochem. Soc.*, 2010, **157**, B1263-B1268.
51. Y. Garsany, I. L. Singer and K. E. Swider-Lyons, *J. Electroanal. Chem.*, 2011, **662**, 396-406.
52. H. Harima, *J. Phys. Chem. Solids*, 2002, **63**, 1035-1038.
53. H. J. Koo, M. H. Whangbo and B. J. Kennedy, *J. Solid State Chem.*, 1998, **136**, 269-273.
54. R. Mani, M. Fischer, J. E. Joy, J. Gopalakrishnan and M. Jansen, *Solid State Sci.*, 2009, **11**, 189-194.
55. M. Tachibana, Y. Kohama, T. Shimoyama, A. Harada, T. Taniyama, M. Itoh, H. Kawaji and T. Atake, *Physical Review B*, 2006, **73**, 193107.
56. J. Suntivich, K. J. May, H. A. Gasteiger, J. B. Goodenough and Y. Shao-Horn, *Science*, 2011, **334**, 1383-1385.
57. B. Hammer and J. K. Nørskov, in *Adv. Catal.*, ed. H. K. Bruce C. Gates, Academic Press, 2000, pp. 71-129.
58. I. S. Shaplygin and V. B. Lazarev, *Materials Research Bulletin*, 1973, **8**, 761-766.
59. A. W. Sleight, *Materials Research Bulletin*, 1971, **6**, 775-780.
60. A. W. Sleight and J. L. Gillson, *Materials Research Bulletin*, 1971, **6**, 781-784.
61. Y. Leng, G. Chen, A. J. Mendoza, T. B. Tighe, M. A. Hickner and C. Wang, *J. Am. Chem. Soc.*, 2012, **134**, 9054-9057.
62. L. Xiao, S. Zhang, J. Pan, C. Yang, M. He, L. Zhuang and J. Lu, *Energy & Environmental Science*, 2012, **5**, 7869.
63. M. Faraj, M. Boccia, H. Miller, F. Martini, S. Borsacchi, M. Geppi and A. Pucci, *Int. J. Hydrogen Energy*, 2012, **37**, 14992-15002.
64. W. Sheng, H. A. Gasteiger and Y. Shao-Horn, *J. Electrochem. Soc.*, 2010, **157**, B1529-B1536.
65. J. Parrondo, C. G. Arges, M. Niedzwiecki, E. B. Anderson, K. E. Ayers and V. Ramani, *Rsc Advances*, 2014, **4**, 9875-9879.
66. J. Parrondo and V. Ramani, *J. Electrochem. Soc.*, 2014, **161**, F1015-F1020.

